Int. J. Heat Mass Transfer. Vol. 34, No. 3, pp. 853–861, 1991
Printed in Great Britain

0017-9310/91 \$3.00+0.00

Thermal analysis of shell and tube exchangers with divided-flow pattern

Y. XUAN, B. SPANG and W. ROETZEL
Institute of Thermodynamics, University of the Federal Armed Forces, Holstenhofweg 85, D-2000 Hamburg 70, F.R.G.

(*Received* 1 *December* 1989)

Abstract—Thermal analysis for the divided-flow heat exchanger with an arbitrary number N of tubeside passes is made and corresponding temperature equations are derived. By means of these equations thermal effectiveness, mean temperature difference correction factor and the temperature at a given location on the exchanger surface are calculated. Also, the optimum entrance location of the shellside flow and the influence of the division of the shellside flow upon the pressure loss are discussed.

1. INTRODUCTION

THERE are many industrial process reasons—better balance required between the shellside and the tubeside heat transfer coefficients, vibration problems, more effective use of available shellside pressure drop in low-pressure-drop cases—that lead to the application of shell and tube exchangers with various configurations. One of such exchangers is called the divided-flow heat exchanger, designated as the 'J-type' in TEMA standards [1]. Provided the shellside heat transfer resistance is not the limiting factor and entrance as well as exit losses are neglected, the shellside pressure loss is reduced to approximately one eighth of that of the conventional shell and tube heat exchanger.

Gardner [2] derived equations for the mean temperature difference of one tube pass divided-flow heat exchangers. The analysis of two tube pass and one shell pass divided-flow exchangers was made by Kern and Carpenter [3]. Jaw [4] showed a simplified derivation for two tube passes and presented a new derivation for four tube passes. However, all these studies were restricted to the middle entrance of the shellside flow and even distribution of mass flow rate in each half of the exchanger as constant overall heat transfer coefficient U throughout the exchanger.

Heat exchangers with one shell pass and N ($N = 1, 2, \ldots$) tube passes are often referred to as $1-N$ exchangers. The thermal analysis for $1-N$ conventional heat exchangers has been carried out [5]. The purpose of this paper is to present an analysis method for $1-N$ divided-flow heat exchangers with arbitrary NTUs, arbitrary distribution of the mass flow rate on the shellside and variable entrance locations of the shellside flow. The formulas for calculating temperatures of the shellside fluid and of the tubeside fluid in each tube pass, the thermal effectiveness and the mean temperature difference correction factor F will be derived. The related graphs will be made. 1–2 divided-flow exchangers will be taken as an example to be compared with conventional shell and tube exchangers. Also, the pressure loss on the shellside and the optimum entrance location of the shellside flow will be discussed.

2. FORMULATION

Figure 1 shows schematic representations of the heat transfer process in $1-N$ divided-flow heat exchangers. The flow pattern in (a) is designated as $Sc = 1$ and the flow pattern in (b) as $Sc = 2$. Because of the division of the shellside flow, the whole heat transfer region is divided into two subregions, which are designated as subregions e and f, respectively. In the analysis the following assumptions are made:

(1) The shellside fluid is completely mixed at any transverse section. No bypassing and stratification occur.

(2) Piecewise constant heat transfer coefficient: the heat transfer coefficient is assumed to be constant within one pass in each subregion, but it may vary with passes and subregions.

(3) There is no phase change and heat losses are negligible.

(4) The specific heat capacities are constant throughout the exchanger.

As shown in Fig. 1, the origin of the coordinate system is always located on the left of subregion e. To facilitate the derivation, some dimensionless variables and parameters are introduced as follows:

$$x = \frac{l}{L} = \frac{a_i}{A_i} = \frac{a}{A}$$

$$t = \frac{\theta_2 - \theta_2'}{\theta_1' - \theta_2'}, \quad T = \frac{\theta_1 - \theta_2'}{\theta_1' - \theta_2'}$$

$$\beta_e = \frac{\dot{W}_e}{\dot{W}_1}, \quad \beta_f = \frac{\dot{W}_f}{\dot{W}_1}$$

NOMENCLATURE

a	heat transfer surface area along the flow path [m^2]
A	total heat transfer surface area of the exchanger [m^2]
b	constant coefficient
c, d, p, q	constant coefficients
C_j, D_j	eigenvectors
$\mathbf{E}, \mathbf{F}, \mathbf{W}$	coefficient matrices
F	mean temperature difference correction factor
$\mathbf{G}, \mathbf{Y}$	coefficient vectors
h_j, l_j	constant coefficients to be determined
$\mathbf{I}$	unit matrix
l	flow location of fluid [m]
L	length of exchanger [m]
N	number of tube passes
NTU	number of transfer units, $NTU_1 = UA/\dot{W}_1$, $NTU_2 = UA/\dot{W}_2$
P	dimensionless temperature change through the exchanger
ΔP	pressure loss [N m^{-2}]
R	thermal flow rate ratio, $R_1 = \dot{W}_1/\dot{W}_2$, $R_2 = \dot{W}_2/\dot{W}_1$
Sc	tubeside flow pattern shown in Fig. 1
$t_{i,i+1}$	intermediate temperature of the tubeside fluid
Δt_m	true mean temperature difference
$\Delta t_{\log}$	logarithmic mean temperature difference
t	dimensionless temperature of the tubeside fluid
T	dimensionless temperature of the shellside fluid
$\mathbf{T}$	dimensionless temperature vector
U	overall heat transfer coefficient [W m^{-2} K^{-1}]
$\dot{W}$	thermal flow rate [W K^{-1}]
x	dimensionless flow path coordinate
z	function defined by equation (49).

Greek symbols

α	constant coefficient
β	division ratio of the shellside flow rate
ε_i	ratio of NTU_i in tube pass i to the overall NTU of the exchanger
θ	temperature [K]
λ	eigenvalue
ρ	parameter
σ	constant coefficient
ϕ	function defined by equation (50)
ω	velocity of fluid [m s^{-1}].

Subscripts

e, E	subregion e
f, F	subregion f
1, s	shellside
2	tubeside
i, j	order number of elements of matrices.

Superscripts

$'$	inlet
$''$	outlet
*	conventional shell and tube exchanger.

$$NTU_1 = \frac{UA}{\dot{W}_1}, \quad NTU_2 = \frac{UA}{\dot{W}_2}$$

$$\varepsilon_i = \frac{(UA)_i}{UA} = \frac{(NTU_1)_i}{NTU_1} = \frac{(NTU_2)_i}{NTU_2}$$

$$P_1 = \frac{\theta'_1 - \theta''_1}{\theta'_1 - \theta'_2}, \quad P_2 = \frac{\theta''_2 - \theta'_2}{\theta'_1 - \theta'_2}.$$

Obviously, the following relationships are valid:

$$\sum_{i=1}^{N} \varepsilon_i = 1, \quad \beta_e + \beta_f = 1 \tag{1}$$

$$\frac{P_1}{P_2} = \frac{NTU_1}{NTU_2} = \frac{\dot{W}_2}{\dot{W}_1} = R_2. \tag{2}$$

At the entrances and the exits of the exchangers one has

$$T' = 1, \quad t'_1 = 0, \quad T'' = 1 - P_1, \quad t''_N = P_2. \tag{3}$$

In this paper, the theory for divided-flow exchangers is extended by introduction of the NTU-ratio ε_i [5], which allows for different surface areas and heat transfer coefficients among the tube passes. Further, the thermal flow rate ratio β is introduced, which allows for arbitrary division of the shellside flow rate between two subregions. The shellside fluid is divided at any ratio β_e and its entrance may be located at different positions. According to the heat balance and by means of the above-defined dimensionless variables, temperature equations can be obtained for each subregion. For subregion e ($0 \leqslant x \leqslant x_e$)

$$(UA)_i(T_e - t_{ei}) = \pm(-1)^i \dot{W}_2 \frac{dt_{ei}}{dx} \quad (i = 1, 2, \ldots, N) \tag{4}$$

$$\frac{dT_e}{dx} = \pm \sum_{i=1}^{N} (-1)^i \frac{\dot{W}_2}{\dot{W}_1 \beta_e} \frac{dt_{ei}}{dx}. \tag{5}$$

For subregion f ($x_e \leqslant x \leqslant 1$)

$$(UA)_i(T_f - t_{fi}) = \pm(-1)^i \dot{W}_2 \frac{dt_{fi}}{dx} \quad (i = 1, 2, \ldots, N) \tag{6}$$

$$-\frac{dT_f}{dx} = \pm \sum_{i=1}^{N} (-1)^i \frac{\dot{W}_2}{\dot{W}_1 \beta_f} \frac{dt_{fi}}{dx}. \tag{7}$$

Regarding the relation $\sum_{i=1}^{N} \varepsilon_i = 1$, equations (4) and (5) as well as equations (6) and (7) can be rewritten as

$$\frac{dt_{ei}}{dx} = \pm(-1)^i NTU_2 \varepsilon_i (T_e - t_{ei}) \quad (i = 1,2,\ldots,N) \tag{8}$$

$$\frac{dT_e}{dx} = \frac{NTU_1}{\beta_e} T_e - \frac{NTU_1}{\beta_e} \sum_{i=1}^{N} \varepsilon_i t_{ei} \tag{9}$$

and

$$\frac{dt_{fi}}{dx} = \pm(-1)^i NTU_2 \varepsilon_i (T_f - t_{fi}) \quad (i = 1,2,\ldots,N) \tag{10}$$

$$\frac{dT_f}{dx} = -\frac{NTU_1}{\beta_f} T_f + \frac{NTU_1}{\beta_f} \sum_{i=1}^{N} \varepsilon_i t_{fi} \tag{11}$$

where the minus sign $(-)$ and the positive sign $(+)$ of sign $(\pm)$ in the above-mentioned equations are valid for tube flow pattern $Sc = 1$ and for tube flow pattern $Sc = 2$, respectively, which are shown in Fig. 1.

To solve these $(2+2N)$ linear ordinary differential equations of the first order, the corresponding $(2+2N)$ boundary conditions are needed. The concrete expressions of the conditions are dependent on some factors, such as the tube pass number N (odd or even) and the tubeside flow pattern. Table 1 gives the tubeside boundary conditions and Table 2 the shellside.

In matrix notation the homogeneous system of equations (8) and (9) appear in the form

$$\frac{d\mathbf{T}_E}{dx} = \mathbf{E}\mathbf{T}_E \tag{12}$$

where $\mathbf{T} = (t_{e1}, t_{e2}, \ldots, t_{eN}, T_e)^T$ and $\mathbf{E}$ is a coefficient matrix with order $(N+1)$, the elements of which are given as follows:

$$e_{ij} = \begin{cases} 0 & i \neq j \\ \pm(-1)^{i+1} NTU_2 \varepsilon_i & i = j \end{cases} \quad i,j = 1,2,\ldots,N$$

$$e_{i,N+1} = \pm(-1)^i NTU_2 \varepsilon_i \quad i = 1,2,\ldots,N$$

$$e_{N+1,j} = \begin{cases} -\dfrac{NTU_1 \varepsilon_j}{\beta_e} & j = 1,2,\ldots,N \\ \dfrac{NTU_1}{\beta_e} & j = N+1. \end{cases}$$

Similarly, the homogeneous system consisting of equations (10) and (11) can also be formed as

$$\frac{d\mathbf{T}_F}{dx} = \mathbf{F}\mathbf{T}_F \tag{13}$$

where $\mathbf{T}_F = (t_{f1}, t_{f2}, \ldots, t_{fN}, T_f)^T$ and $\mathbf{F}$ is also a constant coefficient matrix with order $(N+1)$, the elements of which are given as follows:

$$f_{ij} = \begin{cases} 0 & i \neq j \\ \pm(-1)^{i+1} NTU_2 \varepsilon_i & i = j \end{cases} \quad i,j = 1,2,\ldots,N$$

$$f_{i,N+1} = \pm(-1)^i NTU_2 \varepsilon_i \quad i = 1,2,\ldots,N$$

$$f_{N+1,j} = \begin{cases} \dfrac{NTU_1 \varepsilon_j}{\beta_f} & j = 1,2,\ldots,N \\ -\dfrac{NTU_1}{\beta_f} & j = N+1. \end{cases}$$

Now we will seek a general solution matrix for each subregion by means of eigenvalues and eigenvectors. Assuming $C \exp(\lambda_e x)$ to be a solution of system (12), one has

$$(\mathbf{E} - \lambda_e \mathbf{I})C = 0. \tag{14}$$

In order to obtain a non-zero solution for vector C one must have

$$\det(\mathbf{E} - \lambda_e \mathbf{I}) = 0. \tag{15}$$

This is a polynomial equation of degree $(N+1)$ in λ_e, and hence there are $(N+1)$ roots λ_{ej} $(j = 1,2,\ldots,$

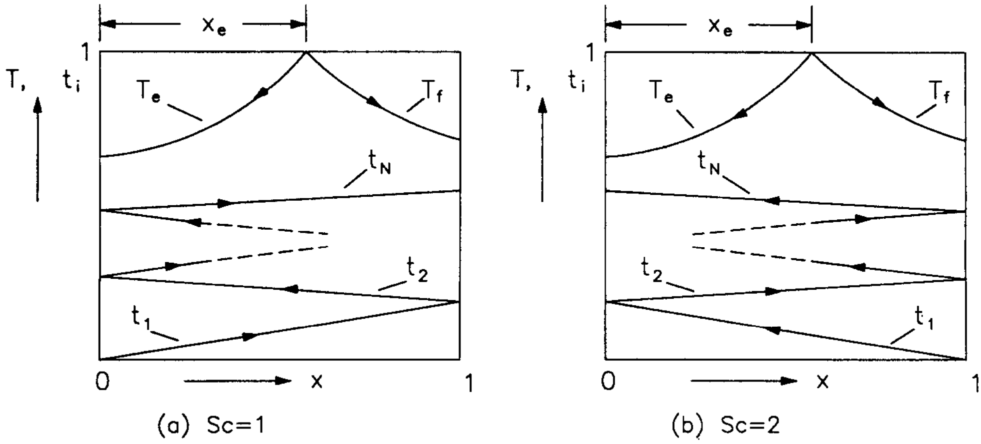

FIG. 1. Thermal scheme of $1-N$ divided-flow heat exchanger.

$N+1$), which are called eigenvalues of matrix $\mathbf{E}$ and the corresponding vectors C_j ($j = 1, 2, \ldots, N+1$) are called eigenvectors of $\mathbf{E}$

$$C_j = (c_{1j}, c_{2j}, \ldots, c_{N+1,j})^{\mathrm{T}}.$$

In the same way, for the homogeneous system (13) there is

$$(\mathbf{F}-\lambda_{\mathrm{f}}\mathbf{I})D = 0 \tag{16}$$

$$\det(\mathbf{F}-\lambda_{\mathrm{f}}\mathbf{I}) = 0. \tag{17}$$

From equations (16) and (17) one can obtain eigenvalues $\lambda_{\mathrm{f}j}$ ($j = 1, 2, \ldots, N+1$) and corresponding eigenvectors D_j ($j = 1, 2, \ldots, N+1$)

$$D_j = (d_{1j}, d_{2j}, \ldots, d_{N+1,j})^{\mathrm{T}}.$$

If matrices $\mathbf{E}$ and $\mathbf{F}$ have distinct eigenvalues, respectively, the unknown temperatures can be described as

$$\mathbf{T}_{\mathrm{E}} = \sum_{j=1}^{N+1} h_j C_j \exp(\lambda_{\mathrm{e}j} x) \tag{18}$$

$$\mathbf{T}_{\mathrm{F}} = \sum_{j=1}^{N+1} l_j D_j \exp(\lambda_{\mathrm{f}j} x) \tag{19}$$

where h_j, l_j ($j = 1, 2, \ldots, N+1$) are constant coefficients to be determined with the boundary conditions given in Tables 1 and 2.

However, in the case that there are multiple eigenvalues, solutions (18) and (19) may not be directly used and they must be corrected. For example, if $\lambda_{\mathrm{e}j}$ is a root of multiplicity m and $\lambda_{\mathrm{f}j}$ is a root of multiplicity n, a solution of forms is suggested [6] to treat this case

$$T_{\mathrm{E}j} = C_j(x)\exp(\lambda_{\mathrm{e}j} x)$$

$$T_{\mathrm{F}j} = D_j(x)\exp(\lambda_{\mathrm{f}j} x)$$

where $C_j(x)$ is a polynomial of degree $(m-1)$ and $D_j(x)$ is a polynomial of degree $(n-1)$

$$C_j(x) = p_0 + p_1 x + p_2 x^2 + \cdots + p_{m-1} x^{m-1} \tag{20}$$

$$D_j(x) = q_0 + q_1 x + q_2 x^2 + \cdots + q_{n-1} x^{n-1}. \tag{21}$$

Substituting equations (20) and (21) into equations (12) and (13) and equating coefficients of x, one can obtain

Table 2. Boundary conditions for $T_{\mathrm{e}}(x)$ and $T_{\mathrm{f}}(x)$

Location	$x = x_{\mathrm{e}} = L_{\mathrm{e}}/L$
$T(x)$	$T_{\mathrm{e}}(x_{\mathrm{e}}) = 1$, $T_{\mathrm{f}}(x_{\mathrm{e}}) = 1$

$$\begin{aligned}
&(\mathbf{E}-\lambda_{\mathrm{e}j}\mathbf{I})p_{m-1} = 0\\
&(\mathbf{E}-\lambda_{\mathrm{e}j}\mathbf{I})p_{m-2} = (m-1)p_{m-1}\\
&(\mathbf{E}-\lambda_{\mathrm{e}j}\mathbf{I})p_{m-3} = (m-2)p_{m-2}\\
&\qquad\vdots\\
&(\mathbf{E}-\lambda_{\mathrm{e}j}\mathbf{I})p_0 = p_1
\end{aligned} \tag{22}$$

$$\begin{aligned}
&(\mathbf{F}-\lambda_{\mathrm{f}j}\mathbf{I})q_{n-1} = 0\\
&(\mathbf{F}-\lambda_{\mathrm{f}j}\mathbf{I})q_{n-2} = (n-1)q_{n-1}\\
&(\mathbf{F}-\lambda_{\mathrm{f}j}\mathbf{I})q_{n-3} = (n-2)q_{n-2}\\
&\qquad\vdots\\
&(\mathbf{F}-\lambda_{\mathrm{f}j}\mathbf{I})q_0 = q_1.
\end{aligned} \tag{23}$$

Since $\det(\mathbf{E}-\lambda_{\mathrm{e}j}) = 0$ in equations (22), the remaining non-homogeneous equations can be solved step by step, provided that the rank of $(\mathbf{E}-\lambda_{\mathrm{e}j}\mathbf{I})$ is equal to the rank of the augmented matrix formed by $(\mathbf{E}-\lambda_{\mathrm{e}j}\mathbf{I})$ with non-homogeneous terms in equations (22). A similar result is also available for equation (23). On finding $C_j(x)$ and $D_j(x)$, one is able to obtain the general solution forms for the case of multiple eigenvalues $\lambda_{\mathrm{e}j}$ or $\lambda_{\mathrm{f}j}$ by substituting $C_j(x)$ for C_j in equation (18) and $D_j(x)$ for D_j in equation (19).

Coefficients h_j and l_j must be determined to derive the particular solution for the original problem. In the light of the boundary conditions given in Tables 1 and 2 as well as equations (18) and (19), a matrix equation with order $(2N+2)$ for these coefficients arises

$$\mathbf{W}\mathbf{Y} = \mathbf{G} \tag{24}$$

where

$$\mathbf{Y} = (h_1, h_2, \ldots, h_{N+1}, l_1, l_2, \ldots, l_{N+1})^{\mathrm{T}}$$

$$\mathbf{G} = (0, 0, \ldots, 0, 1, 1)^{\mathrm{T}}$$

if the boundary conditions for the shellside fluid are taken as the last two equations.

Table 1. Boundary conditions for $t_{\mathrm{e}i}(x)$ and $t_{\mathrm{f}i}(x)$

		$x = 0$	$x = x_{\mathrm{e}} = L_{\mathrm{e}}/L$	$x = 1$
$Sc = 1$	N even	$t_{\mathrm{e}i} = t_{\mathrm{e}i+1} = t_{\mathrm{e}i,i+1}$ $i = 2, 4, \ldots, N-2$ $t_{\mathrm{e}1} = 0$	$t_{\mathrm{e}i} = t_{\mathrm{f}i}$ $i = 1, 2, \ldots, N$	$t_{\mathrm{f}i} = t_{\mathrm{f}i+1} = t_{\mathrm{f}i,i+1}$ $i = 1, 3, \ldots, N-1$
	N odd	$t_{\mathrm{e}i} = t_{\mathrm{e}i+1} = t_{\mathrm{e}i,i+1}$ $i = 2, 4, \ldots, N-1$ $t_{\mathrm{e}1} = 0$	$t_{\mathrm{e}i} = t_{\mathrm{f}i}$ $i = 1, 2, \ldots, N$	$t_{\mathrm{f}i} = t_{\mathrm{f}i+1} = t_{\mathrm{f}i,i+1}$ $i = 1, 3, \ldots, N-2$
$Sc = 2$	N even	$t_{\mathrm{e}i} = t_{\mathrm{e}i+1} = t_{\mathrm{e}i,i+1}$ $i = 1, 3, \ldots, N-1$	$t_{\mathrm{e}i} = t_{\mathrm{f}i}$ $i = 1, 2, \ldots, N$	$t_{\mathrm{f}i} = t_{\mathrm{f}i+1} = t_{\mathrm{f}i,i+1}$ $i = 2, 4, \ldots, N-2$ $t_{\mathrm{f}1} = 0$
	N odd	$t_{\mathrm{e}i} = t_{\mathrm{e}i+1} = t_{\mathrm{e}i,i+1}$ $i = 1, 3, \ldots, N-2$	$t_{\mathrm{e}i} = t_{\mathrm{f}i}$ $i = 1, 2, \ldots, N$	$t_{\mathrm{f}i} = t_{\mathrm{f}i+1} = t_{\mathrm{f}i,i+1}$ $i = 2, 4, \ldots, N-1$ $t_{\mathrm{f}1} = 0$

Matrix $\mathbf{W}$ with $(2N+2)$ order, has elements which depend on the tube pass number, the tubeside flow pattern and the multiplicity of eigenvalues λ_{ej} as well as λ_{fj}. For example, for the case that $Sc = 1$, N is an even number and all eigenvalues are distinct, elements of matrix $\mathbf{W}$ are given as follows:

from $t_{ei} = t_{ei,i+1}$ at $x = 0$, one has

$$w_{ij} = \begin{cases} c_{ij} - c_{i+1,j} & 1 \leqslant j \leqslant N+1 \\ 0 & N+2 \leqslant j \leqslant 2N+2 \end{cases}$$

$$i = 2, 4, \ldots, N-2;$$

from $t_{fi} = t_{fi,i+1}$ at $x = 1$, one has

$$w_{ij} = \begin{cases} 0 & 1 \leqslant j \leqslant N+1 \\ (d_{i,jj} - d_{i+1,jj}) \exp(\lambda_{fjj}) & N+2 \leqslant j \leqslant 2N+2 \end{cases}$$

$$i = 1, 3, \ldots, N-1;$$

from $t_{el} = 0$ at $x = 0$, one has

$$w_{Nj} = \begin{cases} c_{1j} & 1 \leqslant j \leqslant N+1 \\ 0 & N+2 \leqslant j \leqslant 2N+2; \end{cases}$$

from $t_{ei} = t_{fi}$ at $x = x_e$, one has

$$w_{i+N,j} = \begin{cases} c_{ij} \exp(\lambda_{ej} x_e) & 1 \leqslant j \leqslant N+1 \\ -d_{i,jj} \exp(\lambda_{fjj} x_e) & N+2 \leqslant j \leqslant 2N+2 \end{cases}$$

$$i = 1, 2, \ldots, N;$$

from $T_e = 1$ at $x = x_e$, one has

$$w_{2N+1,j} = \begin{cases} c_{N+1,j} \exp(\lambda_{ej} x_e) & 1 \leqslant j \leqslant N+1 \\ 0 & N+2 \leqslant j \leqslant 2N+2; \end{cases}$$

from $T_f = 1$ at $x = x_e$, one has

$$w_{2N+2,j} = \begin{cases} 0 & 1 \leqslant j \leqslant N+1 \\ d_{N+1,jj} \exp(\lambda_{fjj} x_e) & N+2 \leqslant j \leqslant 2N+2 \end{cases}$$

where $jj = j - N - 1$, if $N+2 \leqslant j \leqslant 2N+2$.

Then, $\mathbf{Y}$ can be calculated according to

$$\mathbf{Y} = \mathbf{W}^{-1}\mathbf{G}. \tag{25}$$

So far the temperatures $T_e(x)$, $T_f(x)$, $t_{ej}(x)$ and $t_{fj}(x)$ ($j = 1, 2, \ldots, N$) are determined. Thus, the outlet temperatures of T_e and T_f appear in forms

$$T''_e = T_e(x=0), \quad T''_f = T_f(x=1) \tag{26}$$

and the final outlet temperature of the shellside fluid is

$$T'' = \frac{\dot{W}_e T_e(0) + \dot{W}_f T_f(1)}{\dot{W}_1} = \beta_e T_e(0) + \beta_f T_f(1) \tag{27}$$

and the temperature change of the shellside fluid in the divided-flow heat exchanger is

$$P_1 = 1 - T'' = 1 - (\beta_e T_e(0) + \beta_f T_f(1)). \tag{28}$$

Therefore, the final temperature change of the tubeside fluid through the exchanger (called the thermal effectiveness) can be obtained

$$P_2 = \frac{P_1 \dot{W}_1}{\dot{W}_2} = (1 - \beta_e T_e(0) - \beta_f T_f(1)) \frac{\dot{W}_1}{\dot{W}_2}$$
$$= \left(1 - \beta_e \sum_{j=1}^{N+1} h_j c_{N+1,j} - \beta_f \sum_{j=1}^{N+1} l_j d_{N+1,j} \exp(\lambda_{fj})\right) \frac{\dot{W}_1}{\dot{W}_2}. \tag{29}$$

Furthermore, the logarithmic mean temperature difference correction factor $F = \Delta t_m / \Delta t_{\log}$ can be expressed as

$$F = \frac{\ln \dfrac{1 - P_2}{1 - P_2 R_2}}{NTU_2 (R_2 - 1)}. \tag{30}$$

Intermediate temperature $t_{i,i+1}$ can be readily determined from the derived temperatures $t_{ei}(x)$ and $t_{fi}(x)$. If N is an even number, $Sc = 1$ and all eigenvalues are distinct, for example, one has

$$t_{i,i+1} = \begin{cases} t_{ei}(0) = \sum_{j=1}^{N+1} h_j c_{ij} & i = 2, 4, \ldots, N-2 \\ t_{fi}(1) = \sum_{j=1}^{N+1} l_j d_{ij} \exp(\lambda_{fj}) & i = 1, 3, \ldots, N-1. \end{cases} \tag{31}$$

3. CALCULATION EXAMPLES

Figure 2 shows NTU_1 and NTU_2 curves as well as F curves in the P_1–P_2 diagram for the 1–3 divided-flow exchanger with the following features: $Sc = 1$, $\varepsilon_1 = 0.3$, $\varepsilon_2 = 0.2$, $\varepsilon_3 = 0.5$, $x_e = 0.5$ and $\beta_e = 0.5$. The advantage of this kind of diagram was discussed in ref. [7]. Figure 3 shows the same type of curves for the 1–2 divided-flow exchanger with the characteristics, such as $Sc = 1$, $\varepsilon_1 = \varepsilon_2 = 0.5$, $x_e = 0.5$ and $\beta_e = 0.5$. Comparing Fig. 2 with Fig. 3, one can find that these curves are almost identical with the same NTU values, if NTUs are less than 3.0. The trend of curves in Fig. 3 is the same as that of curves in Fig.

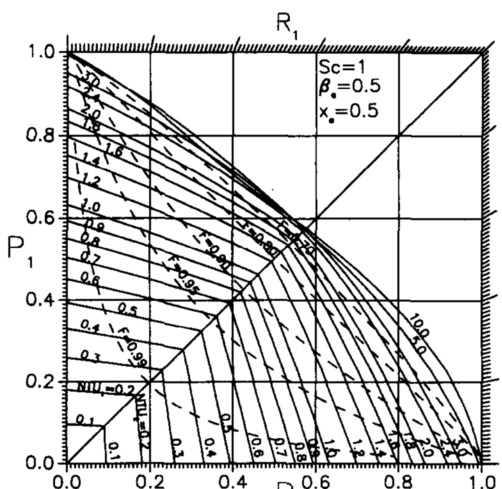

FIG. 2. Three tube passes ($\varepsilon_1 = 0.3$, $\varepsilon_2 = 0.2$, $\varepsilon_3 = 0.5$).

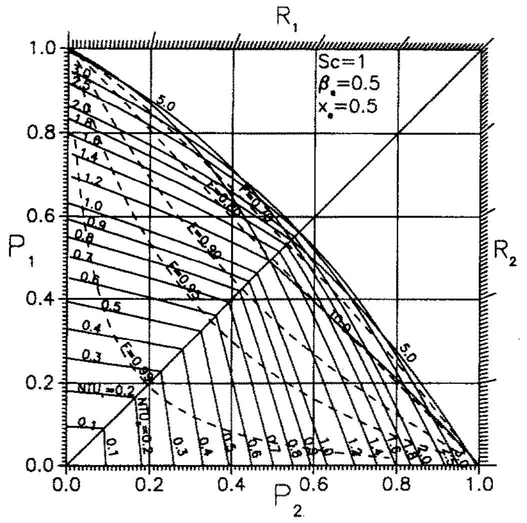

FIG. 3. Two tube passes ($\varepsilon_1 = 0.5$, $\varepsilon_2 = 0.5$).

8 of ref. [4], there are peak values for the thermal effectiveness P_2. Increase of NTU will only cause P_2 to decrease for the divided-flow heat exchangers with even number N of tube passes. This is quite different from the results for a conventional shell and tube heat exchanger (shown in Fig. 4) in which further increase of NTU will not alter the maximum value of P_2. This phenomenon of the divided-flow heat exchangers means that in some portions of the heat transfer surface the dimensionless temperature of the tubeside fluid may exceed the dimensionless temperature of the shellside fluid and reverse heat transfer takes place. This is clearly undesirable. Therefore, peak values should be avoided when such a type of exchanger with an even number N of tube passes is to be designed. However, the reverse heat transfer may be overcome by shifting the entrance location of the shellside fluid.

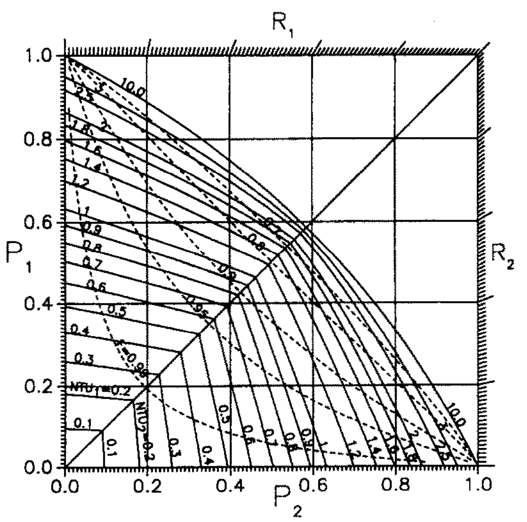

FIG. 4. 1–2 conventional heat exchanger ($\varepsilon_1 = 0.5$, $\varepsilon_2 = 0.5$).

4. PRESSURE LOSS

It is obvious that the ratio of the flow rate in subregion e to the flow rate in subregion f will affect the pressure loss on the shellside. Here the pressure loss ΔP_s means the pressure loss along the shell pass without consideration of baffles. Generally, pressure loss ΔP is formed as [8]

$$\Delta P \sim \omega^\alpha L \tag{32}$$

where

$$\alpha = \begin{cases} 1 & \text{laminar} \\ 1.75 & \text{turbulent.} \end{cases}$$

For a given heat exchanger with the shellside thermal flow rate $\dot{W}_1$, ΔP can be described as

$$\Delta P = \sigma \dot{W}_1^\alpha L. \tag{33}$$

The flow rate on the shellside will be distributed such that

$$\Delta P_s = \Delta P_{se} = \Delta P_{sf} \tag{34}$$

where

$$\Delta P_{se} = \sigma \dot{W}_e^\alpha L_e, \quad \Delta P_{sf} = \sigma \dot{W}_f^\alpha (L - L_e). \tag{35}$$

Therefore, one has

$$L_e \dot{W}_e^\alpha = (L - L_e) \dot{W}_f^\alpha \tag{36}$$

thus

$$\left(\frac{1}{1-\beta_e} - 1\right)^\alpha = \frac{L}{L_e} - 1 \tag{37}$$

or

$$\beta_e = \frac{\left(\dfrac{L}{L_e} - 1\right)^{1/\alpha}}{1 + \left(\dfrac{L}{L_e} - 1\right)^{1/\alpha}}. \tag{38}$$

Equations (37) and (38) show that the ratio β_e cannot be chosen arbitrarily, once the ratio of x_e is given, because equation (34) has to be fulfilled.

In a conventional shell and tube heat exchanger the pressure loss on the shellside is given as

$$\Delta P_s^* = \sigma \dot{W}_1^\alpha L. \tag{39}$$

Comparing equations (35) with equation (39), one can obtain

$$\frac{\Delta P_s}{\Delta P_s^*} = \frac{\Delta P_{se}}{\sigma \dot{W}_1^\alpha L}. \tag{40}$$

If $\Delta P_{se} = \Delta P_{sf}$, equation (40) can be rewritten as

$$\frac{\Delta P_s}{\Delta P_s^*} = \frac{\beta_e^\alpha L_e}{L}. \tag{41}$$

Insertion of equation (38) in equation (41) yields

$$\frac{\Delta P_s}{\Delta P_s^*} = \frac{\beta_e^\alpha}{1+\left(\frac{1}{1-\beta_e}-1\right)^\alpha}. \tag{42}$$

Obviously, the right-hand side of equation (42) is always less than 1.0, which means that the pressure loss on the shellside in the divided-flow exchanger is less than that in the conventional shell and tube exchanger. Equation (41) or (42) can be used for the hydraulic design of such a type of heat exchanger.

In the case where the shellside heat transfer resistance is not the limiting factor, the variation of β_e or x_e does not result in altering NTU_1 as well as NTU_2. Equation (42) can be directly applied to evaluating merits of the divided-flow exchangers because of the same heat transfer characteristics.

If the major heat transfer resistance lies on the shellside, the division of the shellside thermal flow rate $\dot{W}_1$ ($\dot{W}_1 = \dot{W}_e + \dot{W}_f$) will affect the overall heat transfer coefficient U. In general, the heat transfer coefficient on the shellside is proportional to $\omega^{0.6}$ (if the flow on the shellside is turbulent) [9], therefore, UA can be approximately expressed as

$$UA \cong b\dot{W}_e^{0.6}L_e + b\dot{W}_f^{0.6}(L-L_e). \tag{43}$$

In a conventional shell and tube heat exchanger with the same flow rate on the shellside, there is

$$(UA)^* \cong b\dot{W}_1^{0.6}L. \tag{44}$$

Comparison of equation (43) with equation (44) yields

$$\frac{UA}{(UA)^*} = \frac{NTU_1}{NTU_1^*} = \frac{NTU_2}{NTU_2^*} = \beta_e^{0.6}\frac{L_e}{L} + \beta_f^{0.6}\left(1-\frac{L_e}{L}\right). \tag{45}$$

If $\Delta P_{se} = \Delta P_{sf}$, equation (45) can be rewritten as

$$\frac{UA}{(UA)^*} = (1-\beta_e^{0.6}) + \frac{\beta_e^{0.6}-(1-\beta_e)^{0.6}}{1+\left(\frac{1}{1-\beta_e}-1\right)^\alpha}. \tag{46}$$

One should combine equation (42) with equation (46) to analyse the influence of the divided-flow pattern upon the characteristics of shell and tube exchangers, if the shellside heat transfer resistance is controlling.

5. OPTIMUM ENTRANCE

Usually, divided-flow exchangers are designed with the shellside entrance in the middle. This is not the optimum location, regarding the thermal effectiveness and pressure loss. Generally, the optimum entrance location of the shellside fluid depends on factors, such as the number of tube passes, the flow, NTU values, the ratio of the tubeside thermal flow rate to the shellside thermal flow rate, if the maximum thermal effectiveness P_2 is expected. A 1–1 divided-flow exchanger with tube flow pattern $Sc = 2$ is taken as an example to discuss the optimum entrance location of the shellside fluid. According to the previous procedure, the related temperatures can be derived (if $NTU_2 \neq NTU_1/\beta_f$)

$$t_e = c - d\beta_e \exp(\lambda_e x)\frac{NTU_2}{NTU_1}$$

$$T_e = c + d\exp(\lambda_e x)$$

$$t_f = p + q\beta_f \exp(\lambda_f x)\frac{NTU_2}{NTU_1}$$

$$T_f = p + q\exp(\lambda_f x) \tag{47}$$

where

$$q = \frac{1}{\exp(\lambda_f x_e) - \beta_f \exp(\lambda_f)\frac{NTU_2}{NTU_1}}$$

$$p = -\beta_f \exp(\lambda_f) q \frac{NTU_2}{NTU_1}$$

$$d = \frac{1-p-\beta_f \exp(\lambda_f x_e) q \frac{NTU_2}{NTU_1}}{\exp(\lambda_e x_e) + \beta_e \exp(\lambda_e x_e)\frac{NTU_2}{NTU_1}}$$

$$c = 1 - d\exp(\lambda_e x_e)$$

$$\lambda_e = NTU_2 + \frac{NTU_1}{\beta_e}, \quad \lambda_f = NTU_2 - \frac{NTU_1}{\beta_f}.$$

The thermal effectiveness P_2 is expressed as

$$P_2 = t_e(0) = c - d\beta_e\frac{NTU_2}{NTU_1}. \tag{48}$$

From equation (48) the influence of x_e upon P_2 can be analysed. It is worth emphasizing that with changing x_e, the ratio β_e cannot be chosen arbitrarily and β_e is given by equation (38), if $\Delta P_{se} = \Delta P_{sf}$ holds.

Considering equation (38) as a confined condition, introducing a parameter ρ and noting $\beta_f = 1-\beta_e$, one can determine the optimum entrance location x_e. Setting

$$z = P_2 = c - d\beta_e\frac{NTU_2}{NTU_1} \tag{49}$$

$$\phi = \left(1-\frac{1}{1-\beta_e}\right)^\alpha - \frac{L}{L_e} - 1 = 0 \tag{50}$$

one has

$$\frac{\partial z}{\partial x_e} + \rho\frac{\partial \phi}{\partial x_e} = 0 \tag{51}$$

$$\frac{\partial z}{\partial \beta_e} + \rho\frac{\partial \phi}{\partial \beta_e} = 0. \tag{52}$$

The optimum x_e will be determined by solving equations (51) and (52) with the confined condition (50). Figures 5–8 give curves of the thermal effectiveness P_2 vs x_e with such conditions as $\Delta P_{se} = \Delta P_{sf}$, $Sc = 2$ and the turbulent flow on the shellside. Figures 5 and 7 are valid for the case in which the tubeside heat transfer resistance is controlling and Figs. 6 and 8 are suitable

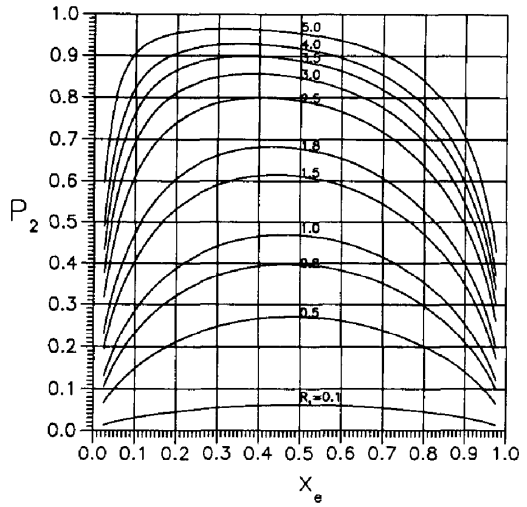

FIG. 5. One tube pass ($NTU_1 = 1.0$, $Sc = 2$, $\Delta P_{se} = \Delta P_{sf}$).

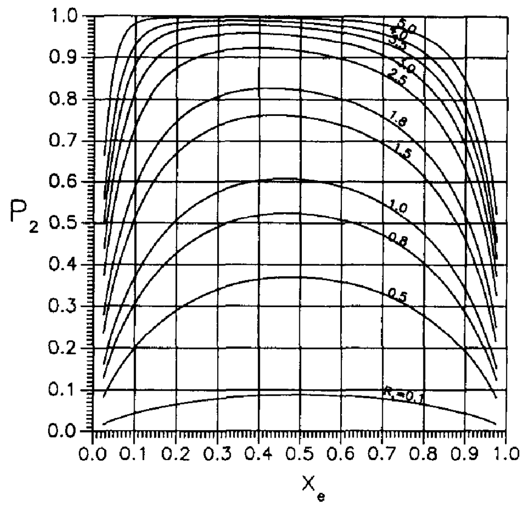

FIG. 7. One tube pass ($NTU_1 = 2.5$, $Sc = 2$, $\Delta P_{se} = \Delta P_{sf}$).

for the case where the major heat transfer resistance lies on the shellside. Preliminary calculations show that the optimum entrance of the shellside flow is not always located at $x_e = 0.5$. It varies with the ratio R_1 and NTU. The value x_e decreases with increase of R_1. If R_1 is greater than 0.5, x_e is smaller than 0.5. If R_1 is constant and NTU changes, the optimum x_e will also deviate from 0.5. With the same R_1 and x_e, the thermal effectiveness P_2 in Figs. 6 and 8 are smaller than those in Figs. 5 and 7 because of the fact that the division of the shellside flow affects the overall heat transfer coefficient, if the major heat transfer resistance is from the shellside flow. With increasing NTU, the deviation of the optimum x_e from 0.5 is smaller, if the overall heat transfer coefficient is mainly contributed by the tubeside heat transfer coefficient. On the contrary, an increase of NTU makes the optimum x_e deviate more from 0.5, if the tubeside heat transfer coefficient occupies the major part of the overall heat transfer coefficient. These curves suggest that designers of such a type of exchangers should reasonably determine the entrance location of the shellside fluid to reach the maximum thermal effectiveness without extra cost. The analysis for the divided-flow with more than one tube pass is similar.

6. CONCLUSION

(1) Heat transfer equations are derived for the $1-N$ divided-flow exchanger with arbitrary ratio β_e, variable entrance location of the shellside fluid and two types of the tubeside flow patterns. These equations can be used to predict the temperatures of the tubeside and shellside fluids at an arbitrary location in the exchangers, thermal effectiveness and correction factor.

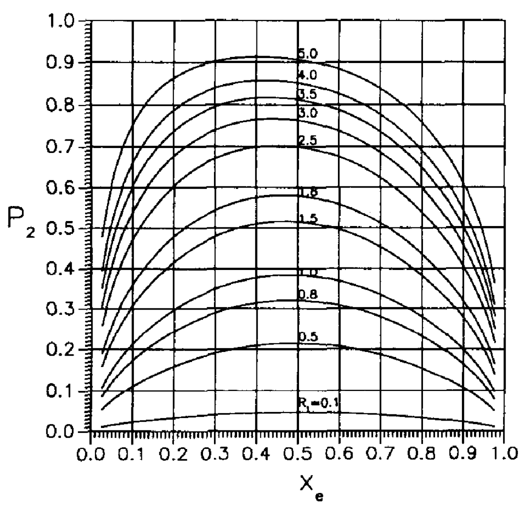

FIG. 6. One tube pass ($NTU_1^* = 1.0$, $Sc = 2$, $\Delta P_{se} = \Delta P_{sf}$).

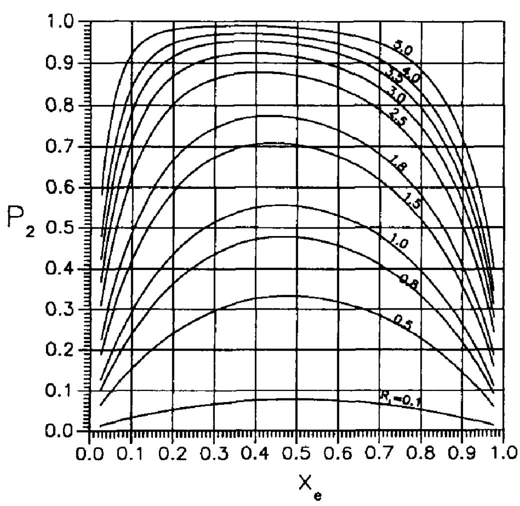

FIG. 8. One tube pass ($NTU_1^* = 2.5$, $Sc = 2$, $\Delta P_{se} = \Delta P_{sf}$).

(2) A few examples are calculated and the graphs of thermal effectiveness P_2 and mean temperature difference correction factor F are made for 1–3 and 1–2 exchangers. Furthermore, a comparison of the divided-flow exchanger with a conventional shell and tube exchanger is carried out. For the former with an even number N of tube passes, there exists a peak value for P_2 and the reverse heat transfer may apparently occur when $NTU > 3.0$.

(3) The influence of the division of the shellside fluid upon the pressure loss and NTU is discussed. The result can be applied to thermal and hydraulic design of the divided-flow heat exchanger.

(4) There exists an optimum entrance location for the shellside fluid. When R_l is greater than 0.5, the optimum entrance x_e deviates from 0.5. Designers should select the optimum entrance for the shellside fluid in order to obtain the maximum thermal effectiveness with lower pressure loss and without extra investment.

REFERENCES

1. *Standards of Tubular Exchanger Manufacturers Association* (6th Edn). TEMA, New York (1978).
2. K. A. Gardner, Mean temperature difference in multipass exchangers, *Ind. Engng Chem.* **33,** 1495–1500 (1941).
3. D. Q. Kern and C. L. Carpenter, True temperature difference in split flow, *Chem. Engng Prog.* **47,** 211–214 (1951).
4. L. Jaw, Temperature relations in shell and tube exchangers having one split-flow shell, *J. Heat Transfer* **89,** 408–416 (1964).
5. W. Roetzel and B. Spang, *Analytisches Verfahren zur thermischen Berechnung mehrgängiger Rohrbündelwärmeübertrager*, Reihe 19, Nr. 18. VDI-Verlag GmbH, Düsseldorf (1987).
6. Tyn Myint-U, *Ordinary Differential Equations*, p. 132. North-Holland, Amsterdam (1978).
7. W. Roetzel and B. Spang, Verbessertes Diagramm zur Berechnung von Wärmeübertragern, *Wärme- und Stoffübertr.* **25,** 259–264 (1990).
8. *VDI-Wärmeatlas*, Ll1–Ll10. VDI-Verlag GmbH, Düsseldorf (1984).
9. J. G. Knudsen and D. L. Katz, *Fluid Dynamics and Heat Transfer*, p. 514. McGraw-Hill, New York (1958).

ANALYSE THERMIQUE DES ECHANGEURS TUBE-CALANDRE AVEC ECOULEMENT DIVISE

Résumé—On fait l'analyse d'un échangeur thermique à écoulement séparé avec un nombre quelconque N de passes dans le tube et les équations correspondantes sont écrites. Au moyen de ces équations sont calculés l'efficacité thermique, le facteur de correction et la température en un point donné de la surface de l'échangeur. On discute de la position optimale de l'entrée de l'écoulement côté calandre et de l'influence sur la perte de pression de la division de l'écoulement côté tube.

UNTERSUCHUNG DES THERMISCHEN VERHALTENS VON ROHRBÜNDELWÄRMEÜBERTRAGERN MIT GETEILTEM MANTELSTROM

Zusammenfassung—Das thermische Verhalten des Rohrbündelwärmeübertragers mit geteiltem Mantelstrom wird für eine beliebige Zahl N von rohrseitigen Durchgängen untersucht und die Gleichungen für den Temperaturverlauf werden hergeleitet. Mit Hilfe dieser Gleichungen können die thermische Leistung, der Korrekturfaktor für die logarithmische mittlere Temperaturdifferenz und die Temperaturen im Apparat berechnet werden. Außerdem werden die optimale Lage des mantelseitigen Eintrittsstutzens und der Einfluß der Aufteilung des Mantelstroms auf den Druckverlust diskutiert.

ТЕРМИЧЕСКИЙ АНАЛИЗ КОЖУХОТРУБНЫХ ТЕПЛООБМЕННИКОВ С РАЗДЕЛЕННЫМИ ПОТОКАМИ

Аннотация—Проведен термический анализ кожухотрубных многоходовых теплообменников с произвольным числом N межтрубных ходов и получены соответствующие температурные соотношения. По этим уравнениям рассчитаны к.п.д., средний поправочный коэффициент разности температур и температура при заданном расположении на поверхности теплообменника. Обсуждается оптимальное расположение входа внешнего потока и влияние разделения внешнего потока на потери давления.